Backbone Mutations in Transmembrane Domains of a Ligand-Gated Ion Channel

ARTICLE *in* CELL · JANUARY 1999

Impact Factor: 32.24 · DOI: 10.1016/S0092-8674(00)80962-9 · Source: PubMed

4 AUTHORS, INCLUDING:

Henry A Lester
California Institute of Technology
434 PUBLICATIONS **22,232** CITATIONS

Cell, Vol. 96, 89–98, January 8, 1999, Copyright ©1999 by Cell Press

Backbone Mutations in Transmembrane Domains of a Ligand-Gated Ion Channel: Implications for the Mechanism of Gating

Pamela M. England,*† Yinong Zhang,*
Dennis A. Dougherty,† and Henry A. Lester*‡
*Division of Biology
†Division of Chemistry and Chemical Engineering
California Institute of Technology
Pasadena, California 91125

Summary

An approach to identify backbone conformational changes underlying nicotinic acetylcholine receptor (nAChR) gating was developed. Specific backbone peptide bonds were replaced with an ester, which disrupts backbone hydrogen bonds at the site of mutation. At a conserved proline residue (αPro221) in the first transmembrane (M1) domain, the amide-to-ester mutation provides receptors with near-normal sensitivity, although the natural amino acids tested other than Pro produce receptors that gate with a much larger EC_{50} than normal. Therefore, a backbone hydrogen bond at this site may interfere with normal gating. In the αM2 domain, the amide-to-ester mutation yielded functional receptors at 15 positions, 3 of which provided receptors with >10-fold lower EC_{50} than wild type. These results support a model for gating that includes significant changes of backbone conformation within the M2 domain.

Introduction

A major challenge in ion channel biology is to describe the dynamic processes associated with gating, for instance the conformational change that couples ligand binding to channel opening. A range of studies, most based on mutagenesis and/or affinity labeling, have identified key residues that define the agonist-binding site and the ion channel. The first ion channel crystal structure has appeared (Doyle et al., 1998), and one can anticipate others. However, these innately static methods call for additional classes of data to reveal the dynamic features of ion channel gating.

If one alters the backbone structure of the protein—replacing the standard peptide backbone with an ester linkage—one can eliminate key hydrogen-bonding interactions that help to establish and maintain secondary structure. A process that involves even subtle changes in backbone conformation/secondary structure would be sensitive to this change. We have found that, indeed, the amide-to-ester change can substantially alter the gating properties of the nicotinic acetylcholine receptor (nAChR). Our results have implications for the gating pathway of the nAChR as well as providing a potentially general tool for studying ion channel conformational changes.

‡To whom correspondence should be addressed (e-mail: lester@caltech.edu).

The nAChR is the prototypical ligand-gated ion channel (Karlin and Akabas, 1995; Edelstein and Changeux, 1998). It is composed of five homologous subunits ($\alpha_2\beta\gamma\delta$ in the embryonic muscle form) arranged in a pentagonal array (Figure 1A). Each of the subunits contains an ~200-residue extracellular domain and four transmembrane domains. The two agonist-binding sites are located primarily on the extracellular domains of the α subunits. The cation-selective pore, which opens in response to agonist binding, is comprised of the M2 domains from each of the subunits (with possible contributions from M1 domains). Notably, the agonist-binding sites are located ~50 Å away from the pore (Herz et al., 1989; Unwin, 1993).

The nonsense suppression technique (Noren et al., 1989) affords the opportunity to incorporate amino acid residues with unnatural side chains into proteins expressed in intact cells. We have reported several studies on nAChR structure–function relations with this method (Nowak et al., 1995; Kearney et al., 1996a; Saks et al., 1996; Zhong et al., 1998). Previously, it was established with in vitro translation systems that α-hydroxy (rather than α-amino) acids can be used to replace the usual peptide backbone bond by an ester, specifically at the target codon (Ellman et al., 1992; Chapman et al., 1997) (Figures 1B and 1C). We now report the first examples of this approach using an in vivo translation system (the *Xenopus* oocyte) and the first applications to an ion channel, the nAChR. We find that nAChR channels with backbone esters express well in *Xenopus* oocytes and produce channels with several hallmarks of normal function.

The amide-to-ester change constitutes a subtle mutation. The size, shape, and chemical nature of the side chain are maintained. This minimizes the ambiguities that necessarily accompany conventional mutagenesis experiments. The most important structural difference introduced by the amide-to-ester change concerns intrastrand backbone hydrogen bonding (i.e., secondary structure), although implications for tertiary and quaternary structure cannot be ruled out. With the exception of proline, amino acids can participate as both hydrogen bond donors and acceptors—a critical aspect in both α helix and β sheet secondary structure (Figure 1C) (Brandl and Deber, 1986; Barlow and Thornton, 1988; Sankararamakrishnan and Vishveshwara, 1992; Yaron and Naider, 1993). An ester, however, cannot serve as a hydrogen bond donor—the critical NH is missing. An ester is still a hydrogen bond acceptor, although a weaker one than an amide. Thus, the amide-to-ester change is expected to highlight the role of specific backbone hydrogen bonds that govern the conformation of the protein near the site of the mutation. To the extent that changes in backbone conformation (i.e., secondary structure) are important in either the static or dynamic aspects of gating, the amide-to-ester mutation should be informative. Earlier work suggests a single amide-to-ester mutation within an α helix disrupts hydrogen bonding so that the protein is destabilized by as much as 1.7 kcal/mol (Koh et al., 1997). Additionally, an ester

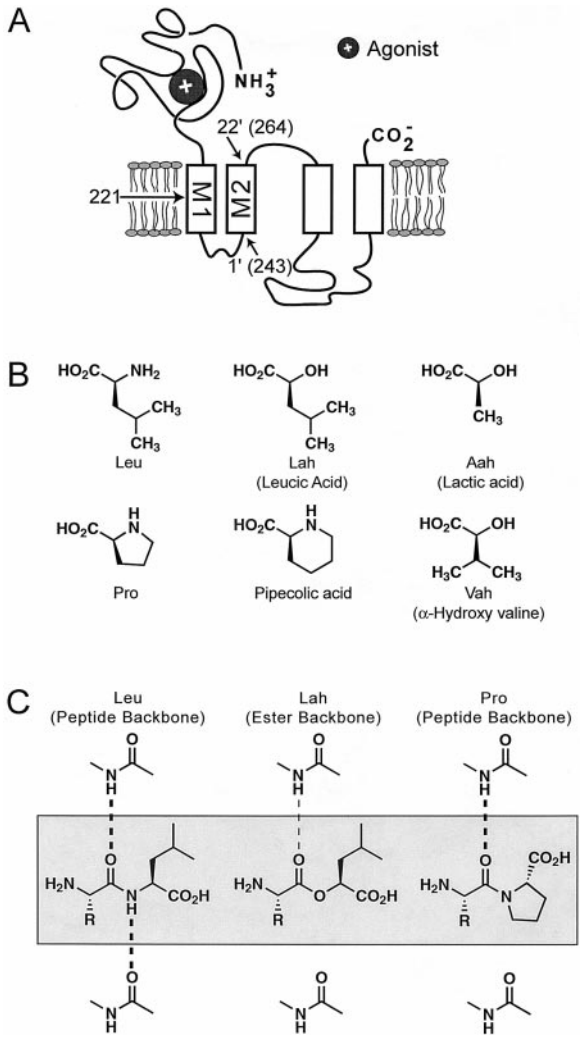

Figure 1. The Nicotinic Acetylcholine Receptor (nAChR) Studied by Backbone Mutagenesis

(A) The probable transmembrane topology of an nAChR subunit and location of the two regions studied. The extracellular agonist-binding site comprises ~200 residues at the N terminus. The Pro-221 residue is thought to lie in the middle of the M1 transmembrane domain. The M2 transmembrane domain extends approximately from positions 243 (abbreviated 1′) to 264 (abbreviated 22′). The five subunits ($\alpha_2\beta\gamma\delta$) are arranged pseudosymmetrically to form the channel pore. The pore is lined primarily by the M2 domains from each of the five subunits.

(B) Structures of six residues (amino acids and α-hydroxy acids) incorporated into the nAChR in this study.

(C) Schematic of the backbone peptide bond versus the backbone ester bond. Structures of a protein chain containing leucine, leucic acid, or proline residues are shown. The drawing emphasizes differences in hydrogen-bonding patterns. Neither the proline residue nor the ester residue formed from leucic acid can serve as a hydrogen bond donor.

and an amide differ in the local dipole moment of the group; that of the amide is significantly larger (Lide, 1990).

Using the amide-to-ester mutation, we sought to address two specific questions regarding the gating of the nAChR. First, what is the role of the M1 proline at position αPro221, a residue that is absolutely conserved throughout the ligand-gated ion channel family? This question has resisted analysis by conventional mutagenesis because only proline itself among natural residues tested produces channels that respond to ACh in the normal range (data on this point are presented in this paper). Furthermore, Gly, Thr, and Phe fail to produce functional responses at the homologous position of the neuronal α7 nAChR (H. Dang and J. M. Patrick, personal communication). The unusual hydrogen bonding properties of proline may account for these results; proline can act only as a hydrogen bond acceptor and not as a donor (Figure 1C). For this reason, Pro residues often have profound influences on static and dynamic aspects of local conformational structure. The hydrogen-bonding pattern of the Xaa–Pro peptide bond is similar to that for an ester, making the αPro221 position an appropriate location for ester incorporation. We find that, indeed, the ester backbone produces functional receptors at position α221.

Second, do the M2 domains undergo secondary structural changes during gating? There are two contrasting suggestions. Based on 9 Å structural studies, Unwin suggested that the M2 domains are kinked α helices that reorient as units upon agonist binding, presumably with little or no change in the intrastrand backbone hydrogen bonds (1995). This view suggests that amide-to-ester backbone mutations in the M2 domains would have minimal effects on channel function. Based on substituted cysteine accessibility mutagenesis (SCAM), Karlin and colleagues suggested that the αM2 domains undergo significant changes in secondary structure, from nonhelical to α-helical, during gating (Karlin and Akabas, 1995; Wilson and Karlin, 1998). This view predicts larger functional effects of amide-to-ester mutations. We find that such mutations do produce measurable changes in EC_{50} throughout the αM2 domains, especially in the region near the extracellular surface of the M2 domains. This is generally more consistent with a model suggesting that parts of the M2 domains undergo changes in backbone conformation during gating.

Results

Receptors with Ester Backbones Have Several Hallmarks of Normal Gating and Function

We charged a nonsense suppressor tRNA (containing a CUA anticodon) with leucic, lactic, or 2-hydroxy-3-methylbutyric acids; these are the α-hydroxy analogs of leucine, alanine, and valine, respectively, and will be termed Lah, Aah, and Vah (Figure 1B). The charged suppressor tRNA was coinjected into *Xenopus* oocytes with mRNA mutated to contain a UAG nonsense codon at the position of interest. Electrophysiological measurements showed that the resulting acetylcholine receptors with esters in the backbone expressed well in oocytes: ACh-induced currents were several μA in amplitude, comparable to or frequently greater than currents produced in our previous studies with unnatural side chains. The nonsense suppression technique is potentially subject to artifacts caused by readthrough of the nonsense (stop) codon or by editing/reacylation of the tRNA with a natural residue, leading to incorporation of this residue

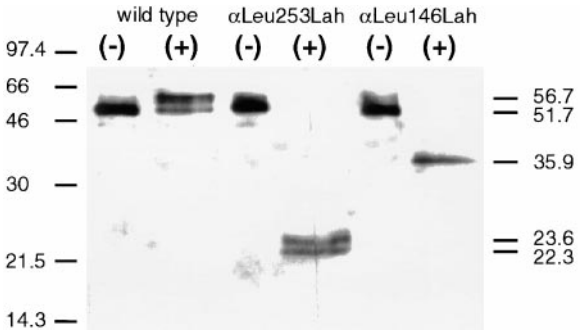

Figure 2. Base-Catalyzed Hydrolysis Shows Site-Specific Formation of an Ester Backbone in the α Subunit of the Nicotinic Receptor Expressed in Oocytes

Hydrolysis of esters formed by incorporation of Lah, an α-hydroxy acid, was studied at two positions. Oocytes were injected with mRNA encoding the wild-type α subunits containing the hemagglutinin epitope and either no additional mutation (lanes 1, 2) or a UAG codon at position 253 (lanes 3, 4) or position 146 (lanes 5, 6), with mRNA encoding wild-type β, γ, and δ subunits, and with THG73 tRNA acylated with Lah. Membranes were isolated and, in lanes marked with (+), also exposed to base. Membranes were then analyzed by gel electrophoresis followed by immunoblotting for the hemagglutinin epitope. Although the wild-type α subunit receptor is not hydrolyzed, the two ester backbone mutant subunits produce lower-MW bands corresponding to the expected MW of the C-terminal hydrolysis fragment.

in proteins (Saks et al., 1996). These artifacts were ruled out in control experiments based on previous detailed tests of the methodology (Saks et al., 1996) as follows: oocytes were injected with the mutated mRNA, but without tRNA, or with the mutated RNA and full-length unacylated tRNA. In these tests, the control ACh responses were <10% of the values recorded in oocytes injected with mRNA and with full-length acylated tRNA.

In addition, Figure 2 presents direct chemical proof that the α-hydroxy acid was incorporated to produce an ester backbone. The experiment was performed with an α subunit that included a hemagglutinin epitope in the intracellular loop between the third and fourth transmembrane domains, a modification that does not measurably alter the dose–response relations of the receptors. Membranes were stripped manually from oocytes expressing nAChR with the usual peptide backbone or from oocytes expressing receptors with targeted ester mutations at either of two sites in the α subunit. A solution of high pH was expected to induce hydrolysis of the ester backbone but not the peptide backbone. After this treatment, gel electrophoresis followed by immunoblotting with the hemagglutinin antibody revealed that, in both cases, the full-length ester band was eliminated and replaced by a peptide fragment with the expected molecular weight, showing that the nonsense suppression procedure resulted in nAChR α subunits with an ester backbone.

An Ester at Residue 221 Allows Gating

The αPro221Leu mutant (α_2Pro221Leu, β, γ, δ) did not produce detectable ACh-induced currents at concentrations as high as 500 μM (Table 1). We also found that Ala or Gly failed to produce functional responses at the αPro221 position (Table 1); and in a previous study, the αPro221Cys mutant was not functional (Akabas and Karlin, 1995). We now show that the αPro221Leu mutant does, however, fold and assemble in the plasma membrane. Figure 3A presents α-bungarotoxin binding data for the αPro221Leu mutant and wild-type receptors. Note that the αPro221Leu receptor displays carbachol-blocked α-bungarotoxin binding, showing that there are surface receptors that contain agonist-binding sites. Similarly, others have shown that the corresponding Pro-to-Leu, -Thr, or -Phe mutation in homomeric α7 receptors allowed surface expression but no function (H. Dang and J. Patrick, personal communication). These data are consistent with the idea that this proline is not necessary for surface expression but is required for robust ACh responses.

Table 1. EC_{50} Values from Macroscopic Dose–Response Studies on Backbone Mutations and Conventional Mutations at a Highly Conserved Pro Residue in the M1 Region

Position	Mutant	EC_{50}, μM	Hill Coefficient
Wild type		47	1.65
αPro221	Lah	88	1.48
	Vah	193	1.36
	Aah	19	2.47
	Pipecolic acid	66	1.78
	Leu	NR	
	Ala	NR	
	Gly	NR	
βPro232	Leu	34	1.46
	Ala	34	1.46
	Gly	99	1.41
γPro229	Leu	59	1.42
	Ala	51	1.42
	Gly	49	1.47
δPro235	Leu	85	1.57
	Ala	70	1.26
	Gly	63	1.25

NR, no response at ACh concentrations up to 500 μM.

To test our hypothesis that the unique hydrogen-bonding properties associated with proline are required for gating, we replaced the peptide backbone at αPro221 with the ester by incorporating Lah. As discussed above, the ester backbone was expected to be a good mimic of the Xaa–Pro peptide backbone. Indeed, the Pro-to-ester mutation produced functional receptors with macroscopic properties similar to those of wild-type receptors (Figure 3B). Dose–response analysis of the αPro221Lah receptors revealed an EC_{50} of 88 μM and a Hill coefficient of 1.48, compared with wild-type values of 47 μM and 1.65. As summarized in Table 1, this proline could also be replaced with the Vah and Aah residues, producing functional ester backbone receptors with EC_{50} values of 19 μM and 193 μM, respectively. We also found that receptors with pipecolic acid, an unnatural amino acid that is structurally homologous to Pro (Figure 1B), were functional (EC_{50} of 66 μM).

Single-channel recordings of the ester-containing receptors were also similar to those of wild-type receptors. We recorded single-channel activities from oocytes expressing the αPro221Lah receptor in response to concentrations of ACh between 1 and 1000 μM. Examples of single-channel openings are shown in Figure 4A. The

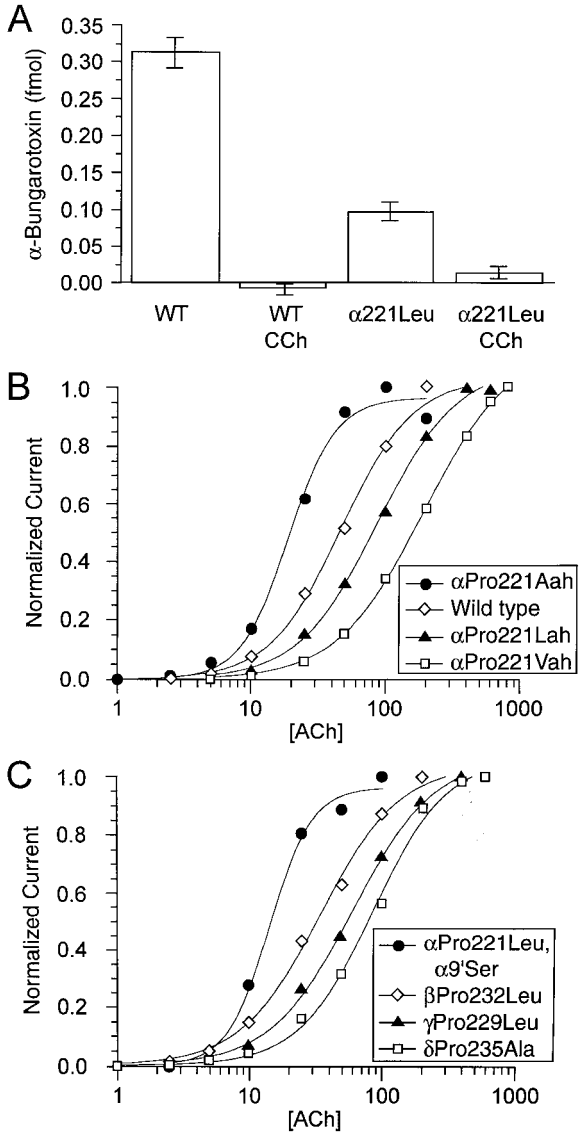

Figure 3. Characteristics of nAChR with Side Chain and Backbone Mutations at α221 and at the Aligning Positions in Other Subunits

(A) α-bungarotoxin binding for the wild-type (WT) and the αPro221-Leu receptor types. Note that the αPro221Leu receptor displays carbachol-blocked α-bungarotoxin binding, showing that there are surface receptors, even though no functional responses were measured.

(B) Dose–response relations are shown for the wild-type nAChR (EC_{50}, 47 μM; Hill coefficient, 1.65) as well as for the three ester backbone mutations: αPro221Lah (88 μM; 1.48), αPro221Vah (193 μM; 1.36), and αPro221Aah (19 μM; 2.47). The lines are least square fits to the dose–response parameters.

(C) Dose–response relations for ACh receptors containing the αPro-221Leu mutation and the aligning mutations at other subunits. The αPro221Leu-αLeu9′Ser receptor has an EC_{50} of 14 μM and a Hill coefficient of ~2. The βPro223Leu, γPro229Leu, and δPro235Ala receptors have EC_{50} values of 34, 59, and 70 μM and Hill coefficients of 1.46, 1.42, and 1.26, respectively.

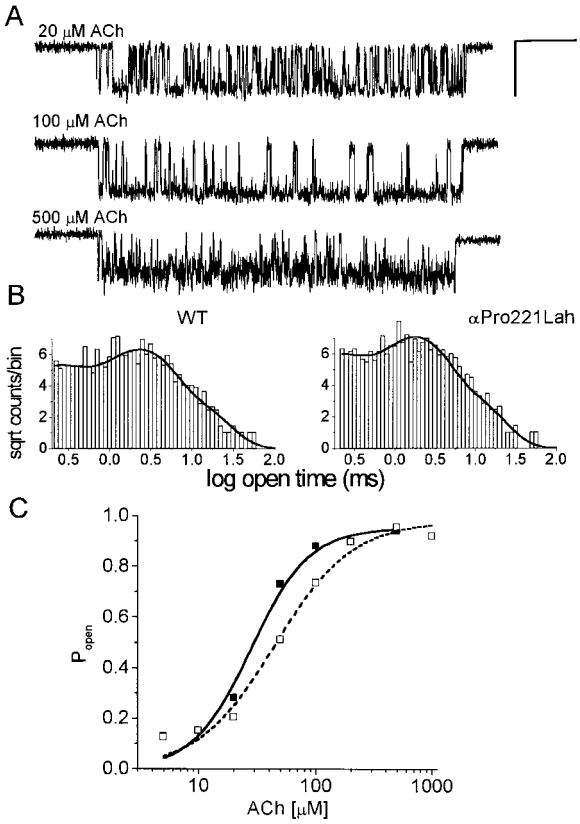

Figure 4. Single-Channel Analysis of the αPro221Lah Mutant

(A) Examples of single-channel openings at several ACh concentrations. Bursts of approximately equal duration are displayed. Calibrations: 25 ms, 5 pA.

(B) Open-channel duration histograms for the wild-type (WT) and αPro221Lah mutant, measured at 5 μM ACh. The time constant for the predominant fraction of open interval distribution was 3.07 ms for the mutant, compared with 3.15 ms for the wild type.

(C) Dose–response analysis. The EC_{50} is 49 μM and the Hill coefficient is 1.47 for the αPro221Lah mutant (open squares), compared with wild-type values of 30 μM and 1.6 (solid squares). The discrepancies in the EC_{50} values between the single-channel and whole-cell recordings may arise from the impact on the amplitudes of macroscopic currents of channel block and desensitization introduced by ACh.

time constant for the predominant fraction of open interval distribution was 3.07 ms for the αPro221Lah mutant, compared with 3.15 ms for the wild type (Figure 4B). The dose–response analysis at the single-channel level is in agreement with values obtained from the macroscopic currents. The EC_{50} of the αPro221Lah mutant is again roughly twice that of the wild-type receptor, and the Hill coefficients are unchanged (1.47 for the αP221 Lah mutant and 1.65 for wild type) (Figure 4B).

The M1 domain in general and αPro221 in particular thus appear to play a crucial role in gating. To explore more fully the role of the M1 domain in gating, the corresponding Pro-to-Leu or -Ala mutations in the β, γ, and δ subunits were constructed. In contrast to the α subunit Pro-to-Leu mutation, the β, γ, and δ mutant receptors with conventional amino acid mutations did gate and functioned with electrophysiological properties similar to wild-type receptors, as shown by the dose–response data plotted in Figure 3C and summarized in Table 1. In a previous study, the βPro232Cys mutant was also functional (Zhang and Karlin, 1997).

To address the question of whether the α subunit is

uniquely sensitive to nonprolyl residues simply because there are two α subunits (Zhang and Karlin, 1997), we designed experiments to examine a receptor containing a single αPro221Leu subunit. This receptor was created by mixing mRNA for the αPro221Leu subunit, the αLeu9′Ser subunit, and wild-type β, γ, and δ subunits. The αLeu9′Ser mutation was included in order to shift the EC_{50} into a measurable region (Revah et al., 1991; Filatov and White, 1995; Labarca et al., 1995). This shift acts independently of mutations at other sites in the protein, such as the ACh-binding site (Kearney et al., 1996a). This combination of subunits was expected to produce a mixture of receptors: $(\alpha Leu9'Ser)_2$, mixed αPro221Leu-αLeu9′Ser, and $(\alpha Pro221Leu)_2$. The $(\alpha Pro221Leu)_2$ receptor is nonfunctional, and the $(\alpha Leu9'Ser)_2$ receptor has an EC_{50} of 1.3 μM, well below the range of ACh concentrations used in this study, so neither of these receptors complicated the analysis. As shown in Figure 3B, the mixed αPro221Leu-αLeu9′Ser receptors were functional, with an EC_{50} of 14 μM and a Hill coefficient of ∼2. This EC_{50} is roughly 6-fold greater than the value for a receptor with α(wild-type)-αLeu9′Ser (Labarca et al., 1995), showing that a Pro-to-Leu mutation in a single α subunit has a significantly larger effect than does the corresponding mutation in the β, γ, or δ subunits. This reasoning also suggests that the $(\alpha Pro221Leu)_2$ receptor has an EC_{50} ∼36-fold larger than the wild-type value, or ∼1800 μM, consistent with the lack of response in our experiments.

Some M2 Domain Backbone Esters Produce Increased Sensitivity

We next turned our attention to the M2 domains, thought to line most of the conduction pore and also to play a prominent role in receptor gating. It was expected that sites involved in backbone hydrogen bond changes during gating would display changes in EC_{50} and other dose–response parameters for the amide-to-ester mutants. We adopt the numbering system in which residue 243 of the α subunit (as well as aligning residues in other subunits) is labeled as the 1′ position (Charnet et al., 1990). This places a highly conserved leucine (α251) at the 9′ position.

The M2 region is rich in Leu and other nonpolar side chains. We performed a series of ester backbone scanning mutagenesis experiments at 15 positions in the α subunit M2 region, as follows (summarized in Table 2). Each of the six wild-type Leu residues (at positions 3′, 8′, 9′, 11′, 15′, and 16′) was replaced in individual experiments with the α-hydroxy acid Lah. Each of the three wild-type Val residues (at positions 13′, 17′, and 19′) was also replaced in individual experiments with the α-hydroxy acid Vah. Because we wished to measure the effects of esters at other positions but did not have the corresponding α-hydroxy acids, we followed a two-step procedure at positions Met-1′, Ile-5′, Ser-10′, and Ile-22′. The wild-type residue was mutated to Leu or Val using the suppression methodology; and in parallel experiments, the appropriate α-hydroxy acid (Lah or Vah) was incorporated at the same position. As a result, we obtained a decisive measure of the change in dose–response relations produced by an amide→ester backbone mutation at 13 of the 22 positions in the M2 region (Figure 5A). At two other positions (2′ and 18′), the hydroxy acid gave functional receptors but the amino acid did not, vitiating the two-step method at these positions.

Table 2. EC_{50} Values (μM) for Backbone Mutations and Conventional Mutations in the M2 Region

Position	Hydroxy Acid	EC_{50}	Amino Acid	EC_{50}
1′Met (243)	Lah	100	Leu	21
2′Thr (244)	Vah	116	Thr	47
3′Leu (245)	Lah	48	Leu*	47
5′Ile (247)	Lah	54	Leu	37
	Vah	70		
8′Leu(250)	Lah	117	Leu*	47
9′Leu(251)	Lah	37	Leu*	47
10′Ser(252)	Lah	4.1	Leu	7.9
11′Leu(253)	Lah	10	Leu*	47
13′Val(255)	Vah	2.3	Val*	47
15′Leu(257)	Lah	18	Leu*	47
16′Leu(258)	Lah	4.6	Leu*	47
17′Val(259)	Vah	67	Val*	47
18′Ile(260)	Lah	92	Ile	47
19′Val(261)	Vah	5.0	Val*	47
22′Ile(264)	Lah	2.4	Leu	7.2

For positions where the wild-type residue is either Leu or Val (marked with an asterisk), the wild-type EC_{50} is given in the last column. For positions where the wild-type residue is neither Leu nor Val, the experiments utilized the two-step strategy described in the text.

Several measures of receptor function are presented in Figure 5. We observed EC_{50} shifts ranging from ∼2- to ∼22-fold produced by ester substitution throughout M2 (Figure 5A). At three positions (13′, 16′, and 19′), the ester mutation provides channels >10× more sensitive to agonist. Notably, these largest EC_{50} shifts occur in a periodic pattern, and there are no sensitivity changes greater than 2.5-fold for positions between 3′ and 10′. The Hill coefficient is also influenced by the conformational changes that accompany gating (Edelstein and Changeux, 1998). This parameter lies between one and two for all the M2 mutants we studied (Figure 5B), suggesting that the open state of the channel is more likely to be associated with the presence of two bound agonist molecules than with a single agonist molecule, as in the wild-type receptor. However, at position 11′ there is a significantly lower Hill coefficient (1.12). Thus, the two equilibrium measures of receptor function, EC_{50} and Hill coefficient, are markedly affected by ester substitution in the region "above" position 10′ in M2.

Single-Channel Currents and Voltage Dependence for Receptors with M2 Domain Esters

We recorded robust single-channel activities from oocytes expressing the αLeu9′Lah receptor (Figure 6). The mutant channel showed characteristics similar to those of the wild-type receptor, such as conductance and clusters of openings at higher ACh concentrations. The open-time duration displayed two components of time constants 1.1 and 5.9 ms, yielding a weighted average open duration of 2.9 ms, close to the wild-type value of 3.3 ms (Figure 4). No channel openings were detected in the absence of ACh. We also recorded single currents from the α11′Lah receptor and found no major differences from the wild-type recordings.

The nicotinic receptor displays voltage-dependent

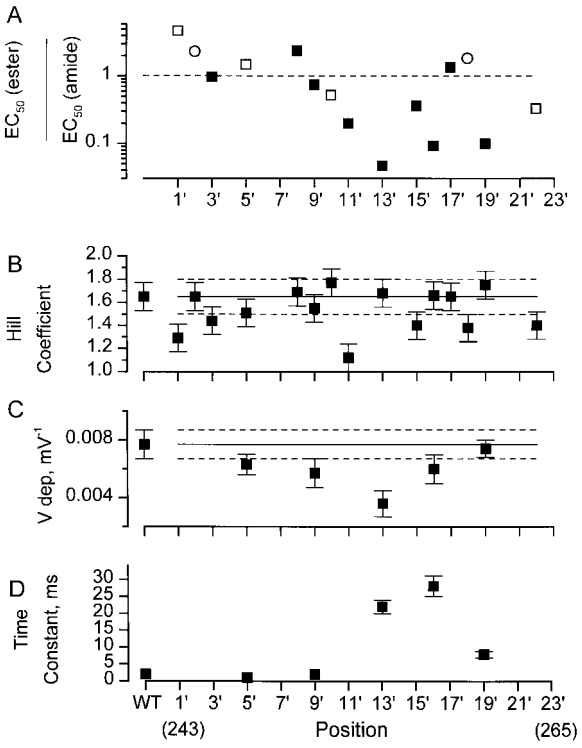

Figure 5. Analysis of Gating for Amide-to-Ester Mutations in the M2 Region

(A) Changes in macroscopic EC_{50} produced by the amide-to-ester mutation at each position. The symbols are based on the data in Table 2. The closed symbols represent mutations from wild-type (WT) Leu or Val residues to Lah or Vah residues. The open squares represent positions where the wild-type residue is neither Leu nor Val; the ratio is (EC_{50} for the Lah mutant)/(EC_{50} for the Leu mutant). The open circles represent positions where the wild-type residue is neither Leu nor Val but the Leu mutation did not express; the ratio is (EC_{50} for the Lah mutant)/(EC_{50} for wild type).

(B) Hill coefficients for the ester backbone mutants. The wild-type value is given at left.

(C) Voltage dependence for responses at five ester backbone mutants. The parameter *a*, defined in the text, is plotted. The wild-type value is given at left.

(D) Voltage-jump relaxation time constants at −120 mV for the five ester backbone mutants studied in (C). The wild-type value is given at left.

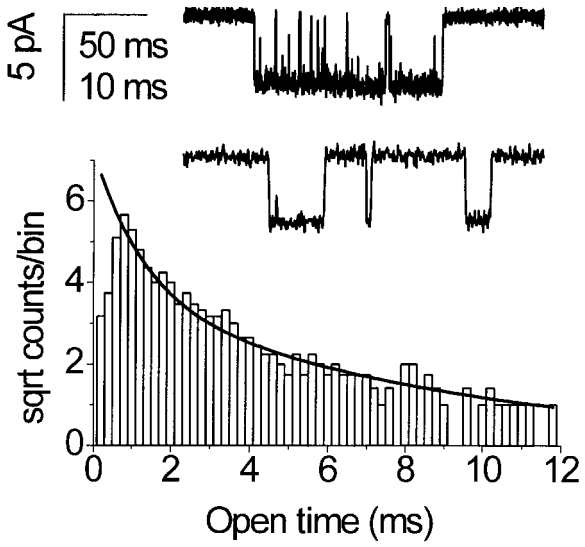

Figure 6. Single-Channel Recordings with an M2 Backbone Mutation: The αLeu9′Lah Receptor

The upper and lower traces show recordings at 100 and 5 μM ACh, respectively. The open-time histogram for 5 μM ACh is shown in the bottom panel. The smooth line represents a fit of open intervals to two components, with time constants of 1.1 ms (63%) and 5.9 ms (37%).

gating, primarily because the open time of the channel increases with hyperpolarization (Magleby and Stevens, 1972a, 1972b; Anderson and Stevens, 1973; Sheridan and Lester, 1977; Auerbach et al., 1996). This voltage dependence presumably arises because the open and closed states differ in a dipole moment that interacts with the membrane field. The ester moiety has a dipole moment of only ~1.7 D, less than half that of the amide (Lide, 1990), which might lead to detectable changes in voltage dependence if the backbone bond reorients within the membrane field during a gating transition. The voltage dependence of gating kinetics can be assessed at either the single-channel or macroscopic level. It was impractical to perform systematic single-channel experiments as a function of membrane potential for all the αM2 ester mutants. We therefore employed voltage-jump relaxation analysis, a technique appropriate for measuring the kinetic and equilibrium aspects of AChR function (Neher and Sakmann, 1975; Sheridan and Lester, 1977).

Figure 7 presents an example of voltage-jump relaxation analysis for the Val19′Vah mutant. The experiment gives the equilibrium level of channel activation at each test potential. This information is abstracted as the parameter *a* in the following equation: $G(V) = G(0)e^{-aV}$, where $G(V)$ is the conductance at membrane potential V. Larger values of *a* indicate greater voltage dependence. Figure 5C shows that the equilibrium voltage dependence is not significantly different from the wild-type value for four of the five positions studied. At position 13′, there is a significantly lower voltage dependence of the equilibrium conductance, suggesting that the receptor has an altered dipole moment in either the open or closed state. It is also possible that the decreased voltage dependence for the backbone mutation at the 13′ position arises from greater participation by monoliganded receptors, which have decreased voltage dependence (Auerbach et al., 1996).

The kinetic information from the voltage-jump experiments is summarized by the relaxation time constants as a function of membrane potential (Figure 7B). Voltage-jump relaxation time constants increase for mutations that decrease EC_{50}, presumably because at low concentrations voltage-jump kinetics are dominated by the channel burst duration. Previous experiments from several laboratories show that increased burst duration underlies the enhanced response to agonist in mutations that decrease EC_{50} (Filatov and White, 1995; Labarca et al., 1995; Sine et al., 1995; Kearney et al., 1996b; Wang et al., 1997). Our methods can resolve only time constants greater than about 2 ms, and the wild-type receptors

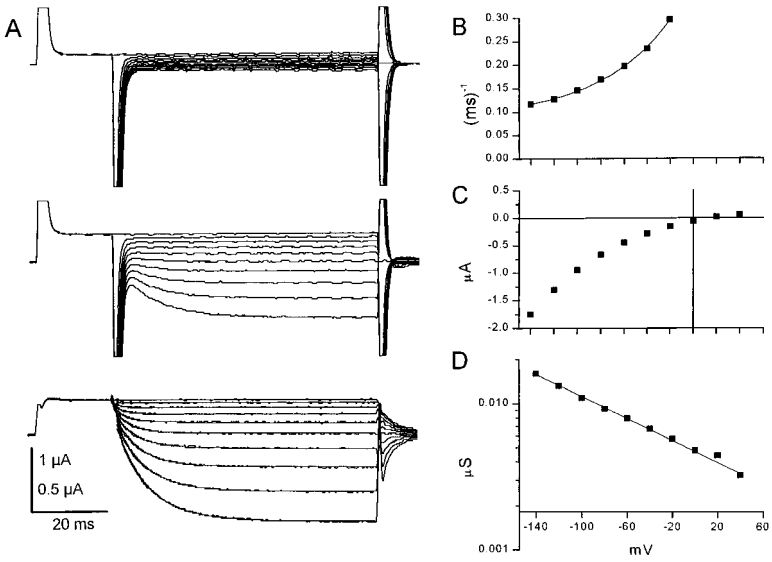

Figure 7. Voltage-Jump Relaxations for the αLeu19′Lah Mutant

(A) The top panel shows voltage-clamp currents in the absence of ACh. The membrane potential was held at −80 mV, stepped to +40 mV for 20 ms, then stepped to test potentials at 20 mV increments between +40 mV and −140 mV. As a result, the ACh-induced conductance relaxed to a new steady-state value over a period of several tens of ms. The middle panel shows the same voltage protocol applied in the presence of 2.5 μM ACh. The subtracted traces, shown in the bottom panel, isolate the voltage-jump relaxation of the ACh-induced current. A single exponential time course was fitted to each of the subtracted traces between −20 mV and −140 mV and superimposes exactly on the traces. Vertical calibrations: 1 μA for the top two panels, 0.5 μA for the bottom panel.

(B) Time constants for the fits as a function of membrane potential.

(C) Steady-state amplitudes of the ACh-induced currents near the end of the test pulses.

(D) Voltage dependence of the steady-state currents. The ACh-induced currents were converted to conductance by dividing by $(V - V_{rev})$, where the reversal potential V_{rev} is +10 mV for this cell. The conductance was plotted on a logarithmic axis and fitted to an exponential function of membrane potential.

had relaxations faster than this value. Comparably fast relaxations were also observed for the 5′ and 9′ amide-to-ester mutations, which do not appreciably decrease EC_{50}. However, the mutations that produced the lowest EC_{50} values also produced observably slow voltage-jump relaxations, for instance at position 19′ in Figure 7. The voltage-jump relaxation time constant for this mutant was ~8 ms at −120 mV. The 13′ and 16′ position also gave rather low EC_{50} values; and the relaxation time constants were appropriately slow, in the range of 20–30 ms (Figure 5D). The amide-to-ester mutations with high agonist sensitivity therefore follow the pattern established for the kinetic properties of nAChR molecules with high agonist affinity caused by conventional side chain mutations: longer open times and increased voltage-jump relaxation time constants.

Discussion

This study introduces amide-to-ester backbone mutations as a probe of the structural changes in ion channel gating. The new approach is made possible by the in vivo nonsense suppression method, applied in this case with α-hydroxy acids. The resulting nAChR channels are characterized by many hallmarks of wild-type function and by differences that fall within the ranges seen with conventional mutagenesis. The dose–response relations in most cases displayed Hill coefficients between one and two; single-channel kinetics and conductance appear nearly normal; and voltage-jump relaxation analyses show kinetics and equilibria within expected ranges.

Asymmetry and Hydrogen Bonding in the M1 Region

We find that a highly conserved proline (Pro-221) in the M1 domain of the α subunits plays a crucial role in nAChR gating. Proline tends to distort ordered secondary structures such as α helices and β sheets (Brandl and Deber, 1986; Barlow and Thornton, 1988; Sankararamakrishnan and Vishveshwara, 1992; Yaron and Naider, 1993). As outlined in the Introduction, this distortion arises at least in part because proline may act only as a hydrogen bond acceptor and not as a donor; in contrast, all other naturally occurring amino acids may participate as both hydrogen bond acceptors and donors (Figure 1C). In one interpretation of our result, then, the highly conserved Pro serves to distort an otherwise straight, α-helical M1 domain in the wild-type receptor. Within the M1 domain, the additional hydrogen bond provided by nonprolyl amino acids may prevent the channel from opening efficiently. The ester backbone substitution produces a hydrogen-bonding pattern resembling that of the proline backbone (Figure 1C), and we find that it produces functional receptors. Consistent with this analysis, the unnatural amino acid pipecolic acid, which also has hydrogen-bonding properties like those of proline, also produces functional receptors at α221.

A similarly crucial role for the M1 Pro residue is not seen in the β, γ, or δ subunits. This is in contrast to the equal and symmetrical contributions that each of the five subunit M2 domains makes to gating, as shown by mutagenesis studies at the Leu9′ site (Filatov and White, 1995; Labarca et al., 1995). The agonist-binding site is primarily, if not exclusively, associated with the α subunits. Our results establish that this asymmetry among the subunits persists to the midpoint of M1 (Pro-221), with the α subunits still playing a unique role. Somewhere between this point and the midpoint of M2 (Leu9′)—a sequence distance of only 30 residues—this asymmetry is lost, and the five subunits contribute equally to gating. One could imagine a gating scheme in which binding to the agonist-binding site in the α

subunit induces movement of the α subunit, and this motion couples directly to the other subunits through contacts in the extracellular domains. However, our data suggest that the signal from the agonist-binding site to the channel gate is confined to the α subunit at least as far as the middle of M1.

Conformational Changes in the M2 Region

The M2 region has been extensively investigated, and two distinct models for receptor gating have been proposed. In one model, the M2 domains of each of the subunits are kinked helices that reorient as rigid units upon agonist binding (Unwin, 1995). In a contrasting second model, the secondary structure within the M2 domains undergoes conformational changes following agonist binding. In particular, the backbone at 8′–10′ is proposed to change from an extended structure in the closed state to an α-helical structure in the open state (Karlin and Akabas, 1995).

Amide-to-ester backbone mutagenesis produced EC_{50} shifts throughout the M2 region, ranging from ~2- to 22-fold. This indicates that changes in backbone structure do occur within the M2 domains upon gating, which would appear to be inconsistent with the rigid unit reorientation model (Unwin, 1995). While generally supporting the conformational change model (Karlin and Akabas, 1995; Wilson and Karlin, 1998), the trends in our data suggest important new details of the model. Large changes are not seen in the 8′–10′ region that was originally proposed to undergo large conformational changes, and only moderate changes occur at the proposed gate region near 2′. Instead, the largest changes in EC_{50} are seen at Val-13′, Leu-16′, and Val-19′. Other large changes are seen in this region, including the decreased voltage dependence at position 13′ and the decreased Hill coefficient at position 11′. Taken together, the present data locate the backbone conformational changes in a region that lies more toward the extracellular face than previously thought. Position 13′ also shows large changes in EC_{50} in conventional mutagenesis studies (Devillers-Thiery et al., 1992; Akabas et al., 1994; Labarca et al., 1995).

We suggest that the differences in the details of the conformational changes proposed here versus the earlier SCAM work reflect differences in the nature of the two methods. The amide-to-ester mutation, in which the side chain structure is held constant, produces less steric perturbation than the Xaa-to-Cys mutation required for SCAM. In addition, SCAM probes accessibility directly and conformational change by inference. The amide-to-ester strategy is of course not perfect either, but it may represent a more direct indicator of secondary structural change. Certainly the 8′–10′ positions experience changes in accessibility to MTS reagents on gating, but we would propose that these are more a consequence of conformational changes higher up the M2 domain that alter their position with respect to the ion channel. We note that positions 13′, 16′, and 19′ are also reactive to SCAM, and both 13′ and 16′ are more reactive toward the SCAM protocol in the open state than the closed state (Akabas et al., 1994). Residue 19′ is equally reactive in both states.

We also note differences between the pattern of sensitivity in our studies and conventional mutagenesis studies. For example, mutations at position 9′ produce dramatic changes in EC_{50} in conventional mutagenesis (Revah et al., 1991; Filatov and White, 1995; Labarca et al., 1995) but not in backbone mutagenesis.

These first results from backbone mutagenesis in an ion channel show that the technique can generate useful data about changes in backbone conformation during gating. Further studies on the nAChR and other channels will define the scope and limitations of the method.

Experimental Procedures

Molecular Biology

The experiments utilized the mouse muscle nAChR α, β, γ, and δ subunits. All mutations were prepared using the polymerase chain reaction to generate cassettes containing the desired point mutation (either TAG or a coding triplet). Cassettes were trimmed with the appropriate restriction enzymes, purified, and ligated into the parent construct (pAMV-PA). The α subunit contained the hemagglutinin epitope at position 347; control experiments verified that this did not detectably change the characteristics of the receptors. Plasmid DNAs were linearized with NotI, and mRNA was transcribed using the Ambion T7 Magic Message Machine kit. The acylated dinucleotides (Nb-Lah-dCA, NVOC-Leu-dCA, and analogs for other residues) were prepared and ligated to THG73 tRNA as previously described (Nowak et al., 1998). Just prior to injection, the photolabile amino protecting group (Nb or NVOC) was removed by irradiating the sample for 5 min at ambient temperature with a 1 kW xenon lamp fitted with WG-335 and UG-11 filters.

Electrophysiology

Stage V–VI *Xenopus* oocytes were isolated and injected one to three times at 24 hr intervals with 50 nl of a 1:1 mixture of mRNA (5–20 ng) and tRNA (25–50 ng). For wild-type or conventional mutant receptors, oocytes were injected once with 50 nl containing 0.13–2.5 ng of mRNA. Electrophysiological recordings were carried out ~24 hr after final injection(s). Macroscopic ACh-induced currents were recorded in response to bath application of the indicated agonist concentrations at −80 mV using a two-electrode voltage clamp configuration. Bath solutions contained 96 mM NaCl, 2 mM KCl, 1 mM $MgCl_2$, and 5 mM Hepes (pH 7.5). Individual dose–response relations were fit to the Hill equation, $I/I_{max} = 1/(1 + \{EC_{50}/[A]\}^{n_H})$, where I is the current for agonist concentration $[A]$, I_{max} is the maximum current, EC_{50} is the concentration to elicit a half-maximum response, and n_H is the Hill coefficient. SEM of EC_{50} measurements was less than 10%; for Hill coefficients, the estimated error is ±0.12. The EC_{50} values in this study encompass a favorable range for quantitative measurements; there is little interference from channel block that occurs at high [ACh] in studies of AChR mutants with EC_{50} values > 200 μM or from spontaneous openings that occur at AChR mutants with EC_{50} values < 1 μM (Labarca et al., 1995). The kinetics of voltage-jump relaxations include contributions from both the opening and closing rates (Adams, 1981; Colquhoun and Hawkes, 1981), and it is therefore important to compare relaxations at comparable levels of receptor activation. We measured voltage-jump relaxations at ACh concentrations equal to half the EC_{50} values.

Cell-attached patch recordings were conducted 24 hr after the final mRNA–tRNA injection. The bath and pipette solution contained (in mM): 115 NaCl, 10 HEPES–NaOH, 1 $CaCl_2$, and 2 KCl (pH 7.4). Membrane potential was held hyperpolarized by 80 mV. The single-channel currents were filtered at 5 kHz (−3 dB; 8-pole Bessel) and stored on a digital data recorder at 48 kHz sampling rate (Neuro Data 384, New York). The data were played back as an analog signal and filtered at 5 kHz and redigitized at 20 kHz. Analysis employed pCLAMP 6 software (Axon Instruments, Foster City, CA). Single-channel clusters were defined by a critical time, which was five times longer than the predominant closed interval component. Dose–response relations were constructed from the probability of

being open (P_{open}) within the clusters and were fitted to the Hill equation.

Bungarotoxin Binding

Oocytes were injected with 50 nl containing mRNA (α:β:γ:δ, 2:1:1:1). For wild-type receptors, oocytes were injected one time with 0.13 ng of mRNA, and for αPro221Leu receptors oocytes were injected three times with 2.5 ng of mRNA. Competition [^{125}I]-α-bungarotoxin/carbachol binding experiments were carried out $\sim$24 hr after final injection in phosphate-buffered saline (1 mM $CaCl_2$) at room temperature. Oocytes were incubated with 5 nM [^{125}I]-α-bungarotoxin with or without 10 mM carbachol for 4 hr, washed several times in ice-cold incubation solution, and counted in a Beckman LS5000 γ-counter.

Hydroxy Acid Synthesis

The hydroxy acids leucic acid (Lah), lactic acid (Aah), and 2-hydroxy-3-methylbutyric acid (Vah) were purchased from Aldrich. The active ester (Nb-Lah-CN) was prepared as previously described (Chapman et al., 1997). The synthesis of the cyanomethyl esters of Aah and Vah will be described elsewhere (P. M. E. and D. A. D., in preparation).

Hydrolysis and SDS-PAGE

Plasma membrane samples were prepared by a manual stripping protocol (Ivanina et al., 1994) with some modifications. To 2.5 ml of a room temperature hypotonic solution (5 mM HEPES, 5 mM NaCl), 25 μl of a 4% SDS solution was added, followed by 10–15 oocytes. After 5–15 min, the vitelline/plasma membranes were removed using a pair of #5 forceps. Isolated membranes were centrifuged at 14,000 rpm for 15 min at 4°C. The pelleted membranes were resuspended in 10 μl of SDS and stored at −80°C. Membrane samples (2 μl) were treated with a solution of 1:1 concentrated ammonium hydroxide/10% SDS for 1.5 hr at room temperature. The solutions were then neutralized by treatment with 30% acetic acid. Untreated samples (2 μl) were allowed to stand at room temperature for the corresponding 1.5 hr. Full-length and cleaved protein products were separated by SDS-PAGE, subjected to Western blot analysis using the anti-hemagglutinin antibody (BAbCO, cat # MMS-101R), and visualized using an ECL detection kit (Amersham).

Acknowledgments

We thank Cesar Labarca for gathering some of the data on conventional mutants in the M1 domain; Hong Dang for sharing unpublished information concerning the α7 receptor; Sonia Pollit and Peter Schultz for samples of leucic acid and pipecolic acid; and members of our laboratory for much discussion. This research was supported by grants from the NIH (grants NS11756 and NS34407) and by National Research Service Awards to P. M. E. and Y. Z.

References

Adams, P.R. (1981). Acetylcholine receptor kinetics. J. Membr. Biol. *58*, 161–174.

Akabas, M.H., Kaufmann, C., Archdeacon, P., and Karlin, A. (1994). Identification of acetylcholine receptor channel-lining residues in the entire M2 segment of the alpha subunit. Neuron *13*, 919–927.

Akabas, M.H., and Karlin, A. (1995). Identification of acetylcholine receptor channel-lining residues in the M1 segment of the α-subunit. Biochemistry *34*, 12496–12500.

Anderson, C.R., and Stevens, C.F. (1973). Voltage-clamp analysis of acetylcholine produced end-plate current fluctuations at frog neuromuscular junction. J. Physiol. (Lond.) *235*, 655–691.

Auerbach, A., Sigurdson, W., Chen, J., and Akk, G. (1996). Voltage dependence of mouse acetylcholine receptor gating: different charge movements in di-, mono-, and unliganded receptors. J. Physiol. *49*, 155–170.

Barlow, D.J., and Thornton, J.M. (1988). Helix geometry in proteins. J. Mol. Biol. *201*, 601–619.

Brandl, C.J., and Deber, C.M. (1986). Hypothesis about the function of membrane-buried proline residues in transport proteins. Proc. Natl. Acad. Sci. USA *83*, 917–921.

Chapman, E., Thorson, J.S., and Schultz, P.G. (1997). Mutational analysis of backbone hydrogen bonds in staphylococcal nuclease. J. Am. Chem. Soc. *119*, 7151–7152.

Charnet, P., Labarca, C., Leonard, R.J., Vogelaar, N.J., Czyzyk, L., Gouin, A., Davidson, N., and Lester, H.A. (1990). An open-channel blocker interacts with adjacent turns of α-helices in the nicotinic acetylcholine receptor. Neuron *2*, 87–95.

Colquhoun, D., and Hawkes, A.G. (1981). Relaxations and fluctuations of membrane currents that flow through drug operated channels. Proc. R. Soc. Lond. B. Biol. Sci. *199*, 231–262.

Devillers-Thiery, A., Galzi, J.L., Bertrand, S., Changeux, J.P., and Bertrand, D. (1992). Stratified organization of the nicotinic acetylcholine receptor channel. Neuroreport *3*, 1001–1004.

Doyle, D., Cabral, J.M., Pfuetzner, R., Kuo, A., Gulbis, J., Cohen, S., Chait, B., and MacKinnon, R. (1998). The structure of the potassium channel: molecular basis of K^+ conduction and selectivity. Science *280*, 69–77.

Edelstein, S.J., and Changeux, J.P. (1998). Allosteric transitions of the acetylcholine receptor. Adv. Protein Chem. *51*, 121–184.

Ellman, J.A., Mendel, D., and Schultz, P.G. (1992). Site-specific incorporation of novel backbone structures into proteins. Science *255*, 197–200.

Filatov, G.N., and White, M.M. (1995). The role of conserved leucines in the M2 domain of the acetylcholine receptor in channel gating. Mol. Pharmacol. *48*, 379–384.

Herz, J.M., Johnson, D.A., and Taylor, P. (1989). Distance between the agonist and noncompetitive inhibitor sites on the nicotinic acetylcholine receptor. J. Biol. Chem. *264*, 12439–12448.

Ivanina, T., Perets, T., Thornhill, W.B., Levin, G., Dascal, N., and Lotan, I. (1994). Phosphorylation by protein kinase A of RCK1 K^+ channels expressed in *Xenopus* oocytes. Biochemistry *33*, 8786–8792.

Karlin, A., and Akabas, M.H. (1995). Toward a structural basis for the function of nicotinic acetylcholine receptors and their cousins. Neuron *15*, 1231–1244.

Kearney, P., Nowak, M.W., Zhong, W., Silverman, S.K., Lester, H.A., and Dougherty, D.A. (1996a). Dose-response relations for unnatural amino acids at the agonist binding site of the nicotinic acetylcholine receptor: tests with novel side chains and with several agonists. Mol. Pharmacol. *50*, 1401–1412.

Kearney, P.C., Zhang, H., Zhong, W., Dougherty, D.A., and Lester, H.A. (1996b). Determinants of nicotinic receptor gating in natural and unnatural side chain structures at the M2 9′ position. Neuron *17*, 1221–1229.

Koh, J.T., Cornish, V.W., and Schultz, P.G. (1997). An experimental approach to evaluating the role of backbone interactions in proteins using unnatural amino acid mutagenesis. Biochemistry *36*, 11314–11322.

Labarca, C., Nowak, M.W., Zhang, H., Tang, L., Deshpande, P., and Lester, H.A. (1995). Channel gating governed symmetrically by conserved leucine residues in the M2 domain of nicotinic receptors. Nature *376*, 514–516.

Lide, D.R. (1990). Handbook of Chemistry and Physics, 71st ed. (Boca Raton: CRC Press). Chap. 9, p. 7.

Magleby, K.L., and Stevens, C.F. (1972a). The effect of voltage on the time course of end-plate currents. J. Physiol. *223*, 151–171.

Magleby, K.L., and Stevens, C.F. (1972b). A quantitative description of end-plate currents. J. Physiol. *223*, 173–197.

Neher, E., and Sakmann, B. (1975). Voltage-dependence of drug-induced conductance in frog neuromuscular junction. Proc. Natl. Acad. Sci. USA *72*, 2140–2144.

Noren, C.J., Anthony-Cahill, S.J., Griffith, M.C., and Schultz, P.G. (1989). A general method for site-specific incorporation of unnatural amino acids into proteins. Science *244*, 182–188.

Nowak, M.W., Kearney, P.C., Sampson, J.R., Saks, M.E., Labarca, C.G., Silverman, S.K., Zhong, W., Thorson, J., Abelson, J.N., Davidson, N., et al. (1995). Nicotinic receptor binding site probed with unnatural amino acid incorporation in intact cells. Science *268*, 439–442.

Nowak, M.W., Gallivan, J.P., Silverman, S.K., Labarca, C.G., Dougherty, D.A., and Lester, H.A. (1998). *In vivo* incorporation of unnatural amino acids into ion channels in a *Xenopus* oocyte expression system. Methods Enzymol. *293*, 504–529.

Revah, F., Bertrand, D., Galzi, J.L., Devillers-Theiry, A., and Mulle, C. (1991). Mutations in the channel domain alter desensitization of a neuronal nicotinic receptor. Nature *353*, 846–849.

Saks, M.E., Sampson, J.R., Nowak, M.W., Kearney, P.C., Du, F., Abelson, J.N., Lester, H.A., and Dougherty, D.A. (1996). An engineered *Tetrahymena* tRNAGln for *in vivo* incorporation of unnatural amino acids into proteins by nonsense suppression. J. Biol. Chem. *271*, 23169–23175.

Sankararamakrishnan, R., and Vishveshwara, S. (1992). Geometry of proline-containing α-helices in proteins. Int. J. Pept. Protein Res. *39*, 356–363.

Sheridan, R.E., and Lester, H.A. (1977). Rates and equilibria at the acetylcholine receptor of *Electrophorus* electroplaques. A study of neurally evoked postsynaptic currents and of voltage-jump relaxations. J. Gen. Physiol. *70*, 187–219.

Sine, S.M., Ohno, K., Bouzat, C., Auerbach, A., Milone, M., Pruitt, J.N., and Engel, A.G. (1995). Mutation of the acetylcholine receptor α subunit causes a slow-channel myasthenic syndrome by enhancing agonist binding affinity. Neuron *15*, 229–239.

Unwin, N. (1993). Nicotinic acetylcholine receptor at 9-Å resolution. J. Mol. Biol. *229*, 1101–1124.

Unwin, N. (1995). Acetylcholine receptor channel imaged in the open state. Nature *373*, 37–43.

Wang, H.L., Auerbach, A., Bren, N., Ohno, K., Engel, A.G., and Sine, S.M. (1997). Mutation in the M1 domain of the acetylcholine receptor α subunit decreases the rate of agonist dissociation. J. Gen. Physiol. *109*, 757–766.

Wilson, G.G., and Karlin, A. (1998). The location of the gate in the acetylcholine receptor channel. Neuron *20*, 1269–1281.

Yaron, A., and Naider, F. (1993). Proline-dependent structural and biological properties of peptides and proteins. Crit. Rev. Biochem. Mol. Biol. *28*, 31–81.

Zhang, H., and Karlin, A. (1997). Identification of acetylcholine receptor channel-lining residues in the M1 segment of the β-subunit. Biochemistry *36*, 15856–15864.

Zhong, W., Gallivan, J.P., Zhang, Y., Li, L., Lester, H.A., and Dougherty, D.A. (1998). From *ab initio* quantum mechanics to molecular neurobiology: a cation-π binding site in the nicotinic receptor. Proc. Natl. Acad. Sci. USA *95*, 12088–12093.